

New Fetal Dose Estimates from ^{18}F -FDG Administered During Pregnancy: Standardization of Dose Calculations and Estimations with Voxel-Based Anthropomorphic Phantoms

Paolo Zanotti-Fregonara¹, Mathieu Chastan², Agathe Edet-Sanson², Ozgul Ekmekcioglu³, Ezgi Basak Erdogan³, Sebastien Hapdey², Elif Hindie¹, and Michael G. Stabin⁴

¹Department of Nuclear Medicine, University Hospital of Bordeaux, Bordeaux, France; ²Department of Nuclear Medicine, Centre Henri Becquerel, Rouen, France; ³Department of Nuclear Medicine, Cerrahpasa Medical Faculty, Istanbul University, Istanbul, Turkey; and ⁴Department of Radiology and Radiological Sciences, Vanderbilt University, Nashville, Tennessee

Data from the literature show that the fetal absorbed dose from ^{18}F -FDG administration to the pregnant mother ranges from $0.5\text{E}-2$ to $4\text{E}-2$ mGy/MBq. These figures were, however, obtained using different quantification techniques and with basic geometric anthropomorphic phantoms. The aim of this study was to refine the fetal dose estimates of published as well as new cases using realistic voxel-based phantoms. **Methods:** The ^{18}F -FDG doses to the fetus ($n = 19$; 5–34 wk of pregnancy) were calculated with new voxel-based anthropomorphic phantoms of the pregnant woman. The image-derived fetal time-integrated activity values were combined with those of the mothers' organs from the International Commission on Radiological Protection publication 106 and the dynamic bladder model with a 1-h bladder-voiding interval. The dose to the uterus was used as a proxy for early pregnancy (up to 10 wk). The time-integrated activities were entered into OLINDA/EXM 1.1 to derive the dose with the classic anthropomorphic phantoms of pregnant women, then into OLINDA/EXM 2.0 to assess the dose using new voxel-based phantoms. **Results:** The average fetal doses (mGy/MBq) with OLINDA/EXM 2.0 were $2.5\text{E}-02$ in early pregnancy, $1.3\text{E}-02$ in the late part of the first trimester, $8.5\text{E}-03$ in the second trimester, and $5.1\text{E}-03$ in the third trimester. The differences compared with the doses calculated with OLINDA/EXM 1.1 were +7%, +70%, +35%, and –8%, respectively. **Conclusion:** Except in late pregnancy, the doses estimated with realistic voxelwise anthropomorphic phantoms are higher than the doses derived from old geometric phantoms. The doses remain, however, well below the threshold for any deterministic effects. Thus, pregnancy is not an absolute contraindication of a clinically justified ^{18}F -FDG PET scan.

Key Words: PET; radiation safety; radiobiology/dosimetry; ^{18}F -FDG; pregnancy; dosimetry

J Nucl Med 2016; 57:1760–1763

DOI: 10.2967/jnumed.116.173294

Scanning a pregnant woman with ^{18}F -FDG remains a rare event in any clinical center, as cancer occurs in about 1 in 1,000 pregnancies (1). However, the number of women injected while pregnant is expected to rise, not only because PET imaging has been steadily growing over the last 20 y, but also because more women become pregnant at a more advanced age, when the incidence of cancers is higher (1).

Thus, to correctly weigh the clinical benefit to the mother against the potential harm to the fetus and for patient counseling, the fetal dosimetry must be known as accurately as possible.

Current dosimetric standards for fetal ^{18}F -FDG dose during pregnancy (2) are based on data obtained from 3 rhesus monkeys in late pregnancy (3). Since the publication of monkey data, 2 small series (1,4) and several case reports (5–9) of ^{18}F -FDG scans of pregnant women have become available in the literature. Although the doses reported in these studies consistently show that the fetal dose is well below the threshold for deterministic effects (10), these doses were obtained with disparate methodologic approaches. For instance, the first cases in early pregnancy were analyzed using a Monte Carlo code and simple geometric models (5,6), whereas in subsequent cases using the dose to the uterus as a proxy was preferred (1,4). Moreover, authors used different assumptions to model the kinetics of the mother's bladder, which is the main contributor to the photon dose to the fetus (1,4). Finally, often the details of the analyses are not fully reported, so that it becomes impossible to reuse the data for further analysis.

Moreover, the dose to the fetus has generally been estimated using the stylized anthropomorphic phantoms (11) implemented in the MIRDOSE (12) and OLINDA/EXM 1.0 software (13). Recently, several sets of more realistic phantoms, based on actual images of humans, have been developed (14). In particular, Segars used the nonuniform rational b-spline modeling technique to obtain a realistic rendering of the human body (15). Building on these data, Stabin and the Society of Nuclear Medicine and Molecular Imaging RADIATION DOSE ASSESSMENT RESOURCE (RADAR) task force developed a complete male and female adult, pediatric, and pregnant woman phantom series (16) using the organ, body, and fetal masses recommended by publication 89 of the International Commission on Radiological Protection (ICRP) (17). These phantoms are implemented in the OLINDA/EXM 2.0 software.

The aim of this study was to establish updated fetal dosimetric standards for ^{18}F -FDG using realistic voxel-based phantoms of pregnant women. To do this, we calculated in a standardized way the

Received Jan. 27, 2016; revision accepted May 4, 2016.

For correspondence or reprints contact: Paolo Zanotti-Fregonara, INCIA UMR-CNRS 5287, Université de Bordeaux, 146 rue Léo Saignat, 33076 Bordeaux Cedex, France.

E-mail: paolo.zanotti-fregonara@chu-bordeaux.fr

Published online Jun. 3, 2016.

COPYRIGHT © 2016 by the Society of Nuclear Medicine and Molecular Imaging, Inc.

fetal dose in a large number of pregnant women imaged with ^{18}F -FDG, including both previously published and new cases.

MATERIALS AND METHODS

Patients

PET images from 17 different women who were imaged for cancer during pregnancy were retrospectively analyzed for this study (Table 1). One woman was scanned twice at 2 different stages of pregnancy (1) and one, here presented for the first time, was expecting twins (Fig. 1). In total, PET data from 19 fetuses were available for analysis. These scans were acquired in different institutions over a time span of many years. Details about the disease staging of the mothers, the type of PET scanners, and the acquisition modalities can be found in the original publications (references are provided in Table 1). The oldest scans were obtained on PET-only cameras ($n = 8$); most scans were acquired with a PET/CT ($n = 9$) and 2 with a modern PET/MRI camera. Attenuation correction, which enables the calculation of radioactivity concentrations in the biologic tissues, was performed with an external radioactive source for PET-only scans, with the CT scan for PET/CT acquisitions, and with the 2-point Dixon technique for the 2 women imaged with PET/MRI. The women were pregnant for 5–34 wk, thus encompassing most of the pregnancy. The average injected activity of ^{18}F -FDG was 303 MBq (range, 174–583 MBq; injected activity ranged from 2.1 to 8.6 MBq/kg). The institutional ethics board approved this retrospective study, and the requirement to obtain informed consent was waived.

Dosimetric Calculations

Pregnancy was divided in 4 periods: early pregnancy (0–10 wk), first trimester (11–13 wk), second trimester (14–26 wk), and third trimester (after 27 wk).

The fetal volume and concentration of radioactivity were derived by manually drawing a region of interest on all slices on which the fetus was visible (or around the whole uterus in early pregnancy). Region-drawing was done directly on the PET images in the PET-only scans or by taking advantage of the anatomic information of the coregistered CT or MR scan, when available. These regions allowed the calculation of the fraction of injected activity concentrated by the fetus (or by the uterus). When the fractions were already available in the original paper, they were used for further analysis. Because any dose estimation to the individual fetal organs would be too uncertain and prone to error, ^{18}F -FDG was supposed to be uniformly distributed in the fetus. The effective half-life of ^{18}F -FDG was conservatively considered to be equal to the physical half-life of ^{18}F (1.83 h). Also, fetal uptake at the time of imaging (about 60 min after injection) was conservatively considered to be reached instantly after injection. The time-integrated activities of the fetuses (or the uterus for the patients in early pregnancy) were combined with those of the mothers' organs, as reported in ICRP publication 106 (Table 2) (18). The dynamic bladder model (12) was used with the following parameters: first fraction of 0.075, with a half-life of 0.2 h, and second fraction of 0.225, with a half-life of 1.5 h (18). The bladder-voiding interval was set at 1 h.

The time-integrated activities were entered into OLINDA/EXM software using both the version 1.1 (17), which contains the old anthropomorphic phantoms of Cristy and Eckerman, and the version 2.0, which contains the more realistic RADAR phantoms (16). For women in early pregnancy, the dose to the uterus was calculated using the anthropomorphic phantom of the nonpregnant woman. For later pregnancy, we used the appropriate pregnant phantoms (Table 1).

TABLE 1
Characteristics of Fetuses and Image-Derived Dosimetry Results

Fetus	Stage of gestation	Mother's weight (kg)	Injected activity (MBq)	Machine	Phantom (trimester)	Time-integrated activity		Dose, Olinda 1 (mGy/MBq)	Dose, Olinda 2 (mGy/MBq)	Reference
						Fraction	(Bq h/Bq)			
1	5 wk	86	296	PET/CT	Nonpregnant	0.0012	0.0030	1.73E-02	1.92E-02	(4)
2	6 wk	68	583	PET	Nonpregnant	0.0036	0.0095	3.14E-02	3.29E-02	(1)
3	8 wk	60	320	PET/CT	Nonpregnant	0.0020	0.0053	2.23E-02	2.39E-02	(5)
4	10 wk	71	296	PET/CT	Nonpregnant	0.0018	0.0046	2.08E-02	2.26E-02	(6)
5	12 wk	58	385	PET/CT	1	0.0006	0.0016	7.25E-03	1.17E-02	(4)
6	~12 wk	77	350	PET	1	0.0010	0.0026	7.70E-03	1.37E-02	(4)
7	18 wk	88	200	PET	2	0.0009	0.0023	3.52E-03	4.98E-03	(1)
8	19 wk	51	348	PET/MRI	2	0.0024	0.0063	4.10E-03	5.72E-03	(4)
9	19 wk	70	296	PET/MRI	2	0.0037	0.0097	4.59E-03	6.34E-03	(4)
10	21 wk	53	181	PET/CT	2	0.0049	0.0129	5.05E-03	6.93E-03	(7)
11	23 wk	59	181	PET	2	0.0078	0.0206	6.17E-03	8.34E-03	(1)
12	25 wk	67	337	PET	2	0.0084	0.0222	6.40E-03	8.64E-03	(1)
13	25 wk	76	188	PET/CT	2	0.0156	0.0412	9.14E-03	1.21E-02	This study
14	25 wk	76	188	PET/CT	2	0.0164	0.0434	9.46E-03	1.25E-02	This study
15	26 wk	81	242	PET/CT	2	0.0129	0.0340	8.10E-03	1.08E-02	(9)
16	28 wk	82	174	PET	3	0.0071	0.0187	3.38E-03	3.36E-03	(1)
17	~28 wk	66	296	PET	3	0.0195	0.0515	6.22E-03	5.62E-03	(4)
18	30 wk	89	229	PET	3	0.0196	0.0518	6.24E-03	5.64E-03	(1)
19	34 wk	95	555	PET/CT	3	0.0192	0.0507	6.15E-03	5.56E-03	(8)

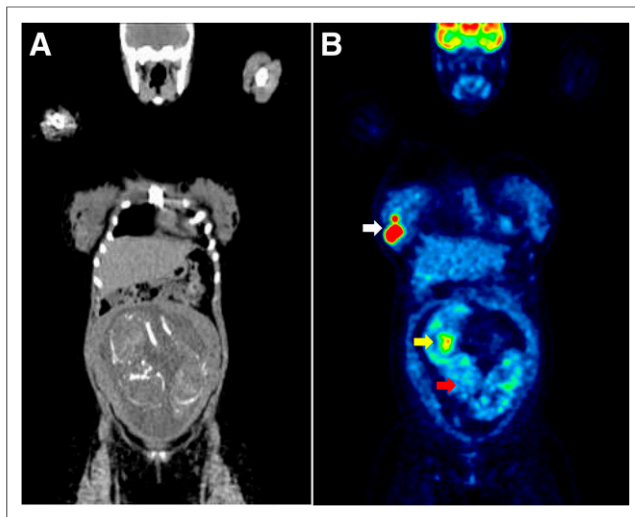


FIGURE 1. Coronal CT (A) and PET (B) image of 29-y-old woman diagnosed with diffuse large B-cell non-Hodgkin lymphoma while expecting twins (about 25 wk pregnant; fetuses 13 and 14 in Table 1). This image was acquired by the Department of Nuclear Medicine of the Henri Becquerel Center in Rouen, France. White arrow points to lymphoma mass in right breast that led to diagnosis. Similarly to all the other late-pregnancy fetuses, uptake in brain (red arrow of fetus on right) is significantly lower than uptake in brain of mother. Yellow arrow points to high ^{18}F -FDG uptake in myocardium of same fetus. Skeletons of the twins are visible on CT scan.

RESULTS

The average fetal doses calculated using the phantoms contained in OLINDA/EXM 1.1 were $2.3\text{E}-02$ mGy/MBq in early pregnancy, $7.5\text{E}-03$ mGy/MBq in the late part of the first trimester, $6.3\text{E}-03$ mGy/MBq in the second trimester, and $5.5\text{E}-03$ mGy/MBq in the third trimester. Fetal self-dose increased progressively with the size of the fetus, ranging from about 10% during the first trimester to about 40% at the end of pregnancy. With OLINDA/EXM 2.0, the doses were $2.5\text{E}-02$ mGy/MBq in early pregnancy, $1.3\text{E}-02$ mGy/MBq in the late part of the first trimester, $8.5\text{E}-03$ mGy/MBq in the second trimester, and $5.1\text{E}-03$ mGy/MBq in the third trimester. Thus, the differences compared with the doses calculated with the old geometric phantoms were +7%, +70%, +35%, and -8%, respectively (Table 3).

DISCUSSION

The present study sought to establish new standard fetal doses from ^{18}F -FDG administration during pregnancy, using realistic

TABLE 2

Standard Time-Integrated Activities for Mothers' Organs,
Taken from ICRP 106

Organ	Time-integrated activity (Bq h/Bq)
Brain	0.21
Heart wall	0.11
Lungs	0.079
Liver	0.13
Rest of the body	1.7

voxel-based anthropomorphic phantoms (16). The value found in early pregnancy ($2.5\text{E}-2$ mGy/MBq) is comparable to the current standard value ($2.2\text{E}-2$ mGy/MBq) estimated from monkey data (2). For the remaining duration of the pregnancy, however, the values from human data were about half to one third those estimated from monkeys (Table 3). Because the ^{18}F -FDG-related fetal dose is well below the threshold for deterministic effects at all stages of pregnancy (10), pregnancy should not be an absolute contraindication to a clinically justified ^{18}F -FDG PET scan (19).

The doses obtained with the new phantoms were similar to those obtained with the old geometric phantoms in early pregnancy (+7%) and in the third trimester (-8%). This is mainly explained by the fact that the mass of the uterus of the nonpregnant woman does not change between the 2 sets of phantoms (80 g), and the mass of the third-trimester fetus is similar (2,961 g for the old phantom and 3,500 g for the new one). By contrast, the fetuses of the first and second trimester are significantly smaller in the new phantoms (85 and 1,114 g, compared with 458 and 1,642 g, respectively), and thus the doses were higher (+70% and +35%, respectively). Dose differences are also partly explained by the different disposition of the organs inside the voxel-based phantoms, which tend to be more closely associated than those in the old phantoms (16).

In particular, the mother's bladder is the main contributor to the fetal dose from photons, especially in early pregnancy (1,4). In this work, we used the bladder model proposed by ICRP publication 106 and standardized the voiding time at 1 h for all cases. Indeed, in most clinical centers patients are scanned about 1 h after injection and are invited to void the bladder just before the scan begins. This voiding time might overestimate the fetal dose in some cases, especially because pregnant women are likely to be asked to void the bladder more often to minimize fetal exposure and, in some institutions, their bladder is drained with a catheter (4). However, a 1-h voiding time is the most likely voiding schedule when the pregnancy is unknown. Therefore, we chose a relatively conservative model.

When a pregnant woman undergoes a PET scan, the transmission scans used for attenuation correction and anatomic imaging add to the total fetal radiation dose. Although the dose from transmission scanning rods is minimal, the dose when using a CT scan is expected to add about 10 mGy to the ^{18}F -FDG dose (1). If PET/MRI machines become more common, they should be the preferred device to image pregnant women. Indeed, PET/MRI machines not only perform attenuation correction without using ionizing radiations, but also allow an accurate delineation of fetal structures (4), which might enable the calculation of fetal absorbed doses at the organ level.

To facilitate comparisons of data from different centers, we suggest that future reports on fetal dosimetry with ^{18}F -FDG use the same approach we used in the present study. This approach would also be helpful with various PET radiopharmaceuticals, particularly those labeled with ^{18}F , that are now increasingly being used (20). At least the fraction of the injected activity concentrated by the fetus should be reported, so that data can be straightforwardly reused for future publications, for example, to test new phantoms.

Finally, this study contains an unexpected finding: even in the most mature fetuses, the fetal brain showed a low ^{18}F -FDG uptake, comparable to that in the soft tissues (Fig. 1). It seems unlikely that the placenta blocks ^{18}F -FDG, because ^{18}F -FDG transport is

TABLE 3
Comparison of New Olinda 2 Values with Values Calculated with Old Anthropomorphic Phantoms Included in Olinda 1

Stage of pregnancy	Values derived from monkeys	Olinda 1 (human data)	Olinda 2 (human data)	Difference*
Early	2.2E-2	2.3E-2	2.5E-2	+7%
First trimester	2.2E-2	7.5E-3	1.3E-2	+70%
Second trimester	1.7E-2	6.3E-3	8.5E-3	+35%
Third trimester	1.7E-2	5.5E-3	5.1E-3	-8%

*(Olinda 2 – Olinda 1)/Olinda 1.
Values derived from nonhuman primates (2) are also provided.

mediated by specific placental transporters (21) and ^{18}F -FDG uptake in the fetal myocardium is always high. Moreover, the blood–brain barrier glucose transporter is conserved in preterm infants (22) although its functional capacity might be lower in the fetal period (23). The most likely explanation is that the brain has low metabolic status in utero. Indeed, there is some evidence that the ^{18}F -FDG brain metabolism in newborns and infants is also low and that it increases progressively with maturation (24,25).

CONCLUSION

Fetal dosimetry values from ^{18}F -FDG administration during pregnancy, estimated with realistic voxelwise anthropomorphic phantoms, are 2.5E-02 mGy/MBq in early pregnancy, 1.3E-02 mGy/MBq in the late part of the first trimester, 8.5E-03 mGy/MBq in the second trimester, and 5.1E-03 mGy/MBq in the third trimester.

DISCLOSURE

The costs of publication of this article were defrayed in part by the payment of page charges. Therefore, and solely to indicate this fact, this article is hereby marked “advertisement” in accordance with 18 USC section 1734. No potential conflict of interest relevant to this article was reported.

REFERENCES

- Takalkar AM, Khandelwal A, Lokitz S, Lilien DL, Stabin MG. ^{18}F -FDG PET in pregnancy and fetal radiation dose estimates. *J Nucl Med*. 2011;52:1035–1040.
- Stabin MG. Proposed addendum to previously published fetal dose estimate tables for ^{18}F -FDG. *J Nucl Med*. 2004;45:634–635.
- Benveniste H, Fowler JS, Rooney WD, et al. Maternal-fetal in vivo imaging: a combined PET and MRI study. *J Nucl Med*. 2003;44:1522–1530.
- Zanotti-Fregonara P, Laforest R, Wallis JW. Fetal radiation dose from ^{18}F -FDG in pregnant patients imaged with PET, PET/CT, and PET/MR. *J Nucl Med*. 2015;56:1218–1222.
- Zanotti-Fregonara P, Champion C, Trebossen R, Maroy R, Devaux JY, Hindie E. Estimation of the beta plus dose to the embryo resulting from F-18-FDG administration during early pregnancy. *J Nucl Med*. 2008;49:679–682.
- Zanotti-Fregonara P, Jan S, Taieb D, et al. Absorbed ^{18}F -FDG dose to the fetus during early pregnancy. *J Nucl Med*. 2010;51:803–805.
- Zanotti-Fregonara P, Koroscil TM, Mantil J, Satter M. Radiation dose to the fetus from [^{18}F]-Fdg administration during the second trimester of pregnancy. *Health Phys*. 2012;102:217–219.
- Erdogan EB, Ekmekcioglu O, Vatankulu B, Ergul N, Demir M, Sonmezoglu K. An unknown pregnancy at term detected by a FDG-PET/CT study in a patient with Hodgkin’s lymphoma: a case report. *Rev Esp Med Nucl Imagen Mol*. 2015;34:201–202.
- Calais J, Hapdey S, Tilly H, Vera P, Chastan M. Hodgkin’s disease staging by FDG PET/CT in a pregnant woman. *Nucl Med Mol Imaging*. 2014;48:244–246.
- Stabin MG. Radiation dose concerns for the pregnant or lactating patient. *Semin Nucl Med*. 2014;44:479–488.
- Stabin M, Watson E, Cristy M, et al. *Mathematical Models and Specific Absorbed Fractions of Photon Energy in the Nonpregnant Adult Female and at the End of Each Trimester of Pregnancy*. ORNL Report ORNL/TM-12907. Oakridge, TN: Oak Ridge National Laboratory; 1995.
- Stabin MG. MIRDOSE: personal computer software for internal dose assessment in nuclear medicine. *J Nucl Med*. 1996;37:538–546.
- Stabin MG, Sparks RB, Crowe E. OLINDA/EXM: the second-generation personal computer software for internal dose assessment in nuclear medicine. *J Nucl Med*. 2005;46:1023–1027.
- Xu X, Eckerman KF. *Handbook of Anatomical Models for Radiation Dosimetry*. Boca Raton, FL: Taylor and Francis; 2009.
- Segars J. Development and Application of the New Dynamic NURBS-Based Cardiac-Torso (NCAT) Phantom [dissertation]. Chapel Hill, NC: University of North Carolina. 2001.
- Stabin MG, Xu XG, Emmons MA, Segars WP, Shi C, Fernald MJ. RADAR reference adult, pediatric, and pregnant female phantom series for internal and external dosimetry. *J Nucl Med*. 2012;53:1807–1813.
- International Commission on Radiological Protection (ICRP). *Basic Anatomical and Physiological Data for Use in Radiological Protection: Reference Values*. ICRP publication 89. New York, NY: Elsevier Health; 2003.
- International Commission on Radiological Protection (ICRP). Radiation dose to patients from radiopharmaceuticals: addendum 3 to ICRP publication 53. ICRP publication 106. *Ann ICRP*. 2008;1–197.
- Zanotti-Fregonara P. Pregnancy should not rule out ^{18}F FDG PET/CT for women with cancer. *Lancet*. 2012;379:1948.
- Shao F, Chen Y, Huang Z, Cai L, Zhang Y. Unexpected pregnancy revealed on ^{18}F -NaF PET/CT. *Clin Nucl Med*. 2016;41:e202–e203.
- Baumann MU, Deborde S, Illsley NP. Placental glucose transfer and fetal growth. *Endocrine*. 2002;19:13–22.
- Mantych GJ, Sotelo-Avila C, Devaskar SU. The blood-brain barrier glucose transporter is conserved in preterm and term newborn infants. *J Clin Endocrinol Metab*. 1993;77:46–49.
- Powers WJ, Rosenbaum JL, Dence CS, Markham J, Videen TO. Cerebral glucose transport and metabolism in preterm human infants. *J Cereb Blood Flow Metab*. 1998;18:632–638.
- Chugani HT, Phelps ME, Mazziotta JC. Positron emission tomography study of human brain functional development. *Ann Neurol*. 1987;22:487–497.
- Kinnala A, Suhonen-Polvi H, Aarimaa T, et al. Cerebral metabolic rate for glucose during the first six months of life: an FDG positron emission tomography study. *Arch Dis Child Fetal Neonatal Ed*. 1996;74:F153–F157.



The Journal of
NUCLEAR MEDICINE

New Fetal Dose Estimates from ^{18}F -FDG Administered During Pregnancy: Standardization of Dose Calculations and Estimations with Voxel-Based Anthropomorphic Phantoms

Paolo Zanotti-Fregonara, Mathieu Chastan, Agathe Edet-Sanson, Ozgul Ekmekcioglu, Ezgi Basak Erdogan, Sebastien Hapdey, Elif Hindie and Michael G. Stabin

J Nucl Med. 2016;57:1760-1763.

Published online: June 3, 2016.

Doi: 10.2967/jnumed.116.173294

This article and updated information are available at:

<http://jnm.snmjournals.org/content/57/11/1760>

Information about reproducing figures, tables, or other portions of this article can be found online at:

<http://jnm.snmjournals.org/site/misc/permission.xhtml>

Information about subscriptions to JNM can be found at:

<http://jnm.snmjournals.org/site/subscriptions/online.xhtml>

The Journal of Nuclear Medicine is published monthly.
SNMMI | Society of Nuclear Medicine and Molecular Imaging
1850 Samuel Morse Drive, Reston, VA 20190.
(Print ISSN: 0161-5505, Online ISSN: 2159-662X)

© Copyright 2016 SNMMI; all rights reserved.

The logo for the Society of Nuclear Medicine and Molecular Imaging (SNMMI) consists of the letters 'S', 'N', 'M', and 'I' arranged in a 2x2 grid. Each letter is white and set within a red square. To the right of this grid, the full name of the society is written in a sans-serif font: 'SOCIETY OF NUCLEAR MEDICINE AND MOLECULAR IMAGING'.

SOCIETY OF
NUCLEAR MEDICINE
AND MOLECULAR IMAGING